THE JOURNAL OF PHYSICAL CHEMISTRY C

Article

pubs.acs.org/JPCC

Ab Initio Calculations of Open-Cell Voltage in Li-Ion Organic Radical Batteries

Nicolas Dardenne,[†] Xavier Blase,[‡] Geoffroy Hautier,[†] Jean-Christophe Charlier,[†] and Gian-Marco Rignanese*[,†]

[†]Institute of Condensed Matter and Nanoscience (IMCN), Université catholique de Louvain, B-1348 Louvain-la-Neuve, Belgium

[‡]CNRS and Grenoble-Alpes University, Institut Néel, F-38042 Grenoble, France

ABSTRACT: In the past decade, radical polymers have been confirmed as promising materials for secondary batteries. Thanks to their processability and structure diversity, their electronic properties can be rationally tuned. To this end, quantum-chemical methods could be used to predict the redox properties of new radical molecules and hence guide experiments. Here we test the agreement between theoretical and experimental reduction potentials for various nitroxide radical polymers. A method based on density functional theory is compared with the higher level many-body perturbation theory and to experimental values. The results indicate that this method allows for fast and accurate estimation of the open-cell voltage of these organic radical Li-ion batteries, suggesting that it would be sufficiently robust to extrapolate to theoretically designed nitroxide radicals.

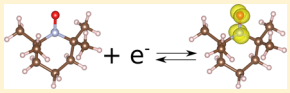

INTRODUCTION

Since the beginning of the 21st century, our mobile society has rapidly become dependent on Li-ion secondary batteries. Nowadays, smart phones, laptops, electric cars, and many other applications require portable, fast rechargeable, and high-capacity power sources. Currently available Li-ion cells are based on inorganic materials, such as $LiCoO_2$ or $LiFePO_4$, which present some drawbacks in terms of cost due to limited natural resources and in terms of waste management due to the toxicity of the constituents.[1] Carbon-based polymers synthesized from metal-free and renewable resources could provide a solution for the development of a green battery.[2−4] In particular, polymers bearing stable redox-active radical pendant groups have generated great expectations.

Well-known radical compounds used in organic radical batteries (ORBs) are nitroxide-based polymers.[5] Poly(2,2,6,6-tetramethyl-1-piperidinyloxy-4-yl methacrylate) (PTMA) is the most common active material, which has already been used as a cathode in Li-ion ORB (Li-ORB). It displays a nearly constant plateau voltage around 3.6 V versus Li/Li^+ with a theoretical capacity of 111 mAh/g.[6] This new type of batteries exhibits high charge/discharge capacity, high charging and discharging rate performance, and long cycle-life.[7] Because of these encouraging characteristics, research on radical polymer batteries has considerably expanded. Recently, Vlad et al. design high-energy and high-power battery electrodes by hybridizing a nitroxide-polymer redox supercapacitor (PTMA) with a Li-ion battery material (LiFePO4).[8] To improve the performance of these supercapacitors, molecular engineering could be applied to various organic radicals to increase the reduction potential and to decrease the molecular mass translating directly into better theoretical capacities. The experimental search for such new materials would greatly benefit from the availability of a fast and accurate quantum chemical method for computing the open-cell voltage and specific energy. Indeed, this would allow for a preliminary screening of theoretically designed radicals, leaving only the most promising candidates for the experimental validation, as previously done in other works (see, e.g., refs 9−14).

A Δ self-consistent field (ΔSCF) procedure based on density functional theory (DFT)[15,16] together with the polarizable continuum model SMD[17] is proposed for meeting the requirements of speed and accuracy. This computational method, based on the difference of total energy between the neutral and cationic radical, is validated on a test set consisting of various nitroxide radical polymers used as cathode materials. The computed OCVs are found to be in good agreement with the experimental values. This approach also correctly reproduces the influence of electron-donating groups on the reduction potentials of nitroxide radicals. The results obtained with the ΔSCF procedure are also corroborated by more accurate, but more time-consuming, calculations performed using many-body perturbation theory (MBPT) in the *GW* approximation.[18−21] The accuracy and speed achieved in the calculations presented here provide a validation for future high-throughput screening of newly designed radicals. In the next section, we begin with a brief summary of the concept of organic radical battery and describe the computational methods used to estimate the OCV.

EXPERIMENTAL BACKGROUND AND THEORETICAL METHODS

A conventional lithium-ion organic radical battery (Li-ORB) is made of metallic lithium anode and of a polymer bearing stable radical groups at the cathode. The two electrodes are immersed in an electrolyte solvent (commonly an aprotic polar solvent containing an electrolyte salt). The first polymer used in a Li-ORB was PTMA (a poly(methacrylate) (PMMA) bearing a

Received: August 13, 2015
Revised: September 21, 2015
Published: September 25, 2015

DOI: 10.1021/acs.jpcc.5b07886
J. Phys. Chem. C 2015, 119, 23373−23378

2,2,6,6-tetramethylpiperdinyloxyl radical (TEMPO)).[6] The TEMPO radical attached to the PMMA backbone (Figure 1a) exhibits a nitroxide center with a localized unpaired

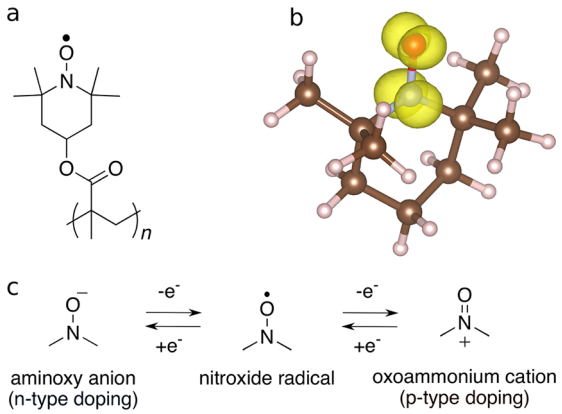

Figure 1. (a) PTMA, (b) spin-up density for radical TEMPO, and (c) redox processes for the nitroxide center.

electron allowing reversible oxidation to form an oxoammonium cation (p-doping) or reversible reduction to an aminoxyl anion (n-doping) (Figure 1c). This one-electron transfer in the redox process allows for high diffusion coefficient and fast electron-transfer efficiency.[22] This characteristic localized unpaired electron can be clearly seen in the computed spin-up density of the radical TEMPO (as illustrated in Figure 1b, computed with Gaussian[23] in DFT with hybrid B3LYP and 6-31+G* basis set) where the SOMO (single occupied molecular orbital) is equally distributed on the nitroxide center.

In the discharged state, the cathode consists of the neutral polymer submerged in the electrolyte solvent (Figure 2). When charging the battery, the nitroxide centers undergo oxidation by the loss of the unpaired electrons and enable the reduction of the lithium cations to metallic state at the anode. At the same time, the electrolyte anions move near the positively charged radicals to balance the electronic transfer. The discharge process is just the reverse reaction. The open-cell voltage reached with the radical TEMPO attached to different polymers [e.g., poly(methacrylate), poly(acetylene), poly(norborene), poly(vinylether), etc.] is ~3.6 V versus Li/Li$^+$.[5] Because the polymer backbone is supposed to have minor influence on the OCV,[5] we assume that the redox reaction takes place on the radical only. Hence, we neglect the role of the backbone and write the discharge reaction as

$$\text{radical}^{+}\text{PF}_{6(\text{solv.})}^{-} + \text{Li}_{(\text{Metal})} \Rightarrow \text{radical}_{(\text{solv.})}^{\bullet} + \text{Li}_{(\text{solv.})}^{+} + \text{PF}_{6(\text{solv.})}^{-} \quad (1)$$

where radical stands for the active pendant group of the polymer (e.g., TEMPO for PTMA) and the superscript dot symbolizes the unpaired electron. The OCV for this reaction 1, also called the redox potential E_{redox}, is the reduction potential of the couple (radical$^+$/radical$^\bullet$) relative to the couple (Li$^+$/Li): $E_{\text{vs Li/Li}^+}$(radical$^+$/radical$^\bullet$).

Other nitroxide radicals linked to various polymers have been successfully tested inside a Li-ORB. The PROXYL (2,2,5,5-tetramethyl-2,5-dihydro-1*H*-pyrrol-1-oxyl-3-yl)[24] and nitronylnitroxide[25] radicals exhibit a similar value of 3.6 V for $E_{\text{vs Li/Li}^+}$. The spirobisnitroxide group presents two nitroxide centers giving rise to two distinct redox processes at 3.66 and 4.43 V versus Li/Li$^+$[26] (Figure 3).

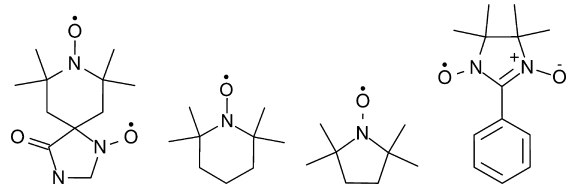

Figure 3. From left to right: spirobisnitroxide, TEMPO, PROXYL, and nitronylnitroxide radicals.

Arylnitroxide radicals have also been tested as potential cathode material but not in a Li-ion battery. To investigate the effect of electron-donating groups on the redox properties of the nitroxide radical, Suga et al. used cyclic voltammetry for characterizing three (*N*-*tert*-butyl-*N*-oxylamino)benzene model compounds.[7] The radicals para-substituted with methoxy, *tert*-butyl, and hydrogen groups (Figure 4) displayed reversible redox potentials $E_{\text{vs Ag/AgCl}}$ of 0.56, 0.75, and 0.83 V, respectively. The reduction potential is shifted with the electron-donating contribution of the methoxy or *tert*-butyl

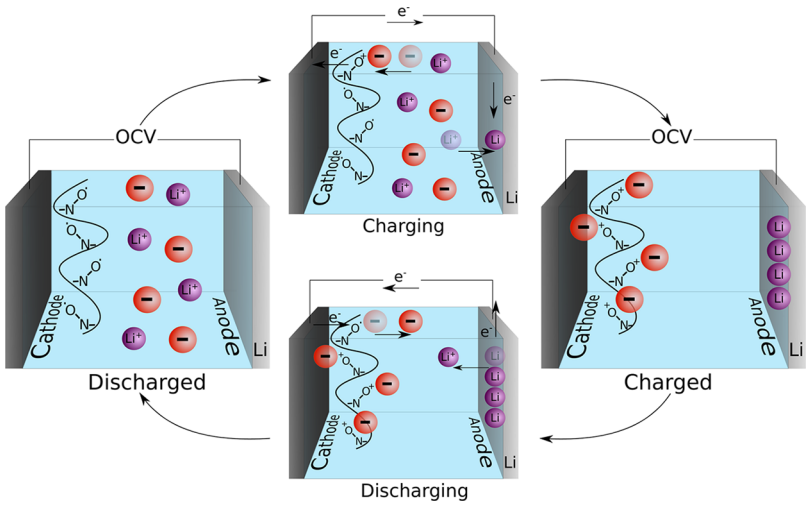

Figure 2. Charging and discharging processes in an organic radical Li-ion battery.

DOI: 10.1021/acs.jpcc.5b07886
J. Phys. Chem. C 2015, 119, 23373−23378

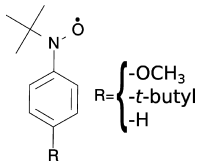

Figure 4. Arylnitroxide radicals with various substituent groups at R position.

substituents, corresponding to changes in the SOMO energy level.

The challenging task of computing redox potentials can be tackled by investigating the two half-reactions taking place at the two electrodes. At the anode, lithium is oxidized

$$\mathrm{Li_{(M)}} \Rightarrow \mathrm{Li_{(solv.)}}^{+} + \mathrm{e}^{-} \tag{2}$$

while, at the cathode, a reduction of the oxidized $PTMA^+$ occurs:

$$\mathrm{radical}^{+}\mathrm{PF_{6(solv.)}}^{-} + \mathrm{e}^{-} \Rightarrow \mathrm{radical_{(solv.)}}^{\cdot} + \mathrm{PF_{6(solv.)}}^{-} \tag{3}$$

The global redox potential is obtained from the absolute reduction potential E_{abs} for both half-reactions as $E_{redox} = E_{abs}(\mathrm{radical}^+/\mathrm{radical}^\bullet) - E_{abs}(\mathrm{Li}^+/\mathrm{Li})$.

The absolute reduction potential can be linked to the Gibbs free-energy change for the reduction reaction $\Delta G_{reduc.}$ (J/mol) by the following equation

$$E_{abs} = \frac{-\Delta G_{reduc.}}{n\mathrm{F}}$$

where n is the number of electrons involved in the reaction and F is the Faraday constant (C/mol). For the reduction at the radical cathode, the Gibbs free-energy change ΔG per molecule is approximated by the total electronic energy change ΔE_{tot} between the oxidized and reduced relaxed states, i.e., the adiabatic ionization. We neglect the zero point motion and thermal and entropic contributions for the radical because they are expected to be very similar in both states and the corresponding terms will cancel each other. Indeed, small changes in the geometry of the radical are expected due to the localized one-electron process. All of the contributions linked to the electron are also ignored because they are expected to be negligibly small.[27] E_{tot} is computed on relaxed structures at the DFT level of theory with different exchange-correlation functionals (B3LYP[28,29] and PBE0[30,31] hybrids and GGA PBE[32,33]) with the 6-31+G* Pople basis set.

The simulations are performed with the Gaussian 09 software,[23] which implements the SMD (Solvation Model Density) polarized continuum model,[17] allowing us to compute the solvation free energy for any solvent. This ΔSCF method can be summarized as

$$E_{abs}(\mathrm{radical}^+/\mathrm{radical}^\bullet) = \frac{-\Delta G^{\circ}}{n\mathrm{F}} \simeq -\underbrace{(E_{tot}^{\mathrm{radical}^\bullet} - E_{tot}^{\mathrm{radical}^+})}_{\mathrm{B3LYP/6\text{-}31+G^*\ SMD}} \tag{4}$$

Similar techniques to predict reduction potential have been used in previous works with organic or inorganic materials.[9,34−42] A review about the computation of liquid-phase reduction potential can be found in ref 27. Our calculations were performed with and without a counteranion to extract the stabilizing effect on the oxidized radical.

To check the validity of the method, we compare the ΔSCF calculations with a higher-level theory. We further perform *GW* calculations of the vertical ionization potential in the gas phase of the studied radicals at their ground-state neutral geometry. Our *GW* calculations are performed at the all-electron level using the Fiesta package that uses Gaussian bases to express both the wave functions and the needed two-body operators.[43−45] To avoid dealing with *GW* calculations on open-shell systems (which are not yet implemented in Fiesta), we define the ionization energy of the neutral radical as the electronic affinity of the related cation. We start from DFT B3LYP or PBE0 Kohn−Sham eigenstates generated by the NWChem code[46] at the maug-cc-pVTZ basis level.[47−49] The Weigend and coworkers auxiliary basis[50] is used in the Fiesta Coulomb-fitting resolution-of-the-identity implementation of the *GW* formalism. Starting from Kohn−Sham states generated with hybrid functionals, we perform "single-shot" perturbative G_0W_0 calculations. Such an approach was advocated in recent papers on small molecules and clusters because it leads to much better results as compared with experiments than G_0W_0 calculations performed on top of Kohn−Sham states generated with (semi)local functionals.[51,52]

To estimate the absolute reduction potential of the anode $E_{abs}(\mathrm{Li}^+/\mathrm{Li})$ in any solvent, we use the up-to-date computed value for the absolute reduction potential for the standard hydrogen electrode [$E^0_{abs}(\mathrm{SHE}) = 4.28$ V[53]] and the experimental value for the relative standard reduction potential of the lithium electrode [$E^0(\mathrm{Li}^+/\mathrm{Li}) = -3.04$ V]. The sum of these two potentials gives the absolute reduction potential of the lithium anode in aqueous solution:

$$E_{abs}^{\mathrm{aqueous}}(\mathrm{Li}^+/\mathrm{Li}) = \underbrace{E^0_{abs}(\mathrm{SHE})}_{\mathrm{computed=4.28\ V}} + \underbrace{E^0(\mathrm{Li}^+/\mathrm{Li})}_{\substack{\mathrm{vs\ SHE}\\ \mathrm{expt.=-3.04\ V=1.24\ V}}} = 1.24\ \mathrm{V} \tag{5}$$

To account for the Gibbs free energy change according to the selected solvent, we add the total electronic energy difference of the lithium cation between the aqueous solution and the solvent to $E_{abs}(\mathrm{Li}^+/\mathrm{Li})$ in water

Table 1. Computed Vertical Ionization Potentials (v. IP) with the G_0W_0 Method on Top of B3LYP and PBE0 Kohn-Sham Wavefunctions, with the ΔSCF/6-31+G* Method with B3LYP, PBE0, and PBE Functional and CCSD Method

	v. IP (eV)[a]					
radicals	G_0W_0@B3LYP	G_0W_0@PBE0	ΔSCF-B3LYP	ΔSCF-PBE0	ΔSCF-PBE	CCSD
TEMPO	7.73	7.63	7.48	7.50	7.12	7.31
PROXYL	7.53	7.44	7.32	7.33	6.96	7.14
nitronylnitroxyl	7.20	7.16	7.10	7.16	6.67	

[a]Computed at the ground-state neutral radical geometry relaxed at the B3LYP/6-31+G* level of theory.

DOI: 10.1021/acs.jpcc.5b07886
J. Phys. Chem. C 2015, 119, 23373−23378

$$E_{abs}(Li^+/Li) = E_{abs}^{aqueous}(Li^+/Li) + \underbrace{(E_{tot}(Li^+_{solvent}) - E_{tot}(Li^+_{aqueous}))}_{B3LYP/6\text{-}31+G^*\ SMD}$$

where the total energy E_{tot} is computed at the same level of theory as for the cathode. In the next section, the results of these simulations are presented and discussed in comparison with the experimental data.

RESULTS AND DISCUSSION

Prior to the computation of the OCV for Li-ORBs, we present the comparison between the more accurate MBPT method and the ΔSCF approach (with B3LYP, PBE0, and PBE functionals) for the vertical ionization in the gas-phase for three nitroxide radicals (Table 1). Within the ΔSCF procedure, the PBE results for the ionization potentials (IPs) are significantly (up to 0.43 eV) smaller than the B3LYP and PBE0 ones, which are nearly identical. One can also notice that the IPs increase with the percentage of exact exchange in the functional. Within the MBPT approach, the G_0W_0@B3LYP or G_0W_0@PBE0 ionization potentials are systematically larger by ∼0.1 to 0.3 eV than the ΔSCF-B3LYP IP values. The apparent overestimation of the G_0W_0 ionization potential has been recently shown to be particularly related to the use of the electronic affinity of the cation as a definition of the ionization potential of the open-shell radical.[54] Clearly, at the nonself-consistent G_0W_0 level, starting from PBE0, instead of B3LYP, eigenstates leads to a closer agreement with the present ΔSCF data, and the use of a functional capturing more exact exchange may further enhance the comparison. A detailed exploration of such issues is beyond the scope of the present paper. Here we limit our MBPT calculations at the present level of refinement that certainly allows us to confirm the trends observed at the DFT level. We have also checked the validity of the reported vertical ionization potentials for the TEMPO and PROXYL radicals using the coupled-cluster singles and doubles (CCSD) approach together with the 6-311+G(2d,p) atomic basis set (Table 1). This choice of a more extended basis set than in DFT calculations is justified by the well-known enhanced sensibility of correlated wave function approaches to basis set effects. The Delta SCF CCSD values have been determined with the Gaussian 09 program.

Table 2. Comparison between Experimental Redox Potentials of the Nitroxylbenzene Derivatives and Their Absolute Reduction Potentials Computed with the ΔSCF@B3LYP Method

functional group	expt. E (V) (vs Ag/AgCl)[a]	computed E_{abs} (V)	
		without counteranion[b]	with counteranion[c]
$-OCH_3$	0.56	4.63	4.58
$-t$-butyl	0.75	4.83	4.78
$-H$	0.83	4.96	4.91

[a]Experimental redox potentials (vs Ag/AgCl) in acetonitrile solution with 0.1 M $(C_4H_9)_4NBF_4$.[7] [b]Computed absolute reduction potential without counteranion. [c]Computed absolute reduction potential with counteranion BF_4^-.

In a second step, we test the ability of the ΔSCF method to predict shifting in the reduction potential according to the functional group attached to the radical. Table 2 illustrates the experimental reduction potentials of the three nitroxylbenzene radicals (Figure 4) and their corresponding computed absolute reduction potentials. The variation according to the substituent groups is correctly reproduced using the proposed theoretical procedure. Experimental data present downward shifts of 0.08 V when replacing the hydrogen with the *tert*-butyl group and of 0.19 V when replacing the *tert*-butyl with a methoxy group. These values can be compared with the computed E_{abs}, which predict shifts of 0.13 and 0.20 V, respectively. The effect of the counteranion has also been studied. A slight and systematic decrease of 0.05 V in the absolute reduction potential can be observed due to the stabilizing effect of the tetrafluoroborate anion on the radical cation.

Finally, in Table 3, we present the results from the ΔSCF method applied to the four nitroxide radicals used in Li-ORB.[22,24−26] These radicals were used as cathode materials in experimental batteries with ethylene carbonate (ETC) and acetonitrile solvents. The SMD parameters for the acetonitrile solvent are directly implemented in Gaussian, and those for the ETC were taken from ref 39. The electrolyte salts were those reported in the literature. From the absolute reduction potential for Li^+/Li in water (1.24 V), we computed a $E_{abs}(Li^+/Li)$ of 1.29 and 1.34 V for ETC and acetonitrile, respectively. Adding these values to the computed absolute reduction potential of the radicals, we get estimated OCVs. We see that the results are in good agreement with the experimental values. For the spirobisniroxide, the simulations predict a gap of 0.75 V between the two redox processes (0.74 V with the counteranion) in perfect agreement with the experimental values (0.75 V). The effect of the counteranion seems to be limited because it lowers the OCV down to a maximum of 0.06 V, which is expected in a solvent with high dielectric permittivity (35.7 for acetonitrile and 89.7 for ETC). Note that the effect of the solvent is very limited. For the TEMPO radical, the computed absolute reduction potentials are 4.86 V in ETC and 4.91 V in acetonitrile; however, the open-cell voltage is 3.57 V in both solvents due to the 0.05 V change in the absolute reduction potential of the lithium.

Table 3. Experimental and Computed Open Cell Voltage with ΔSCF-B3LYP (Comp. OCV.) of Li-ORB for Four Nitroxide Radicals in Acetonitrile (MeCH) and Ethylene Carbonate (ETC) with Lithium Hexafluorophosphate ($LiPF_6$) and Tetrabutylammonium Perchlorate $(R)_4NClO_4$ Salts

radical	solvent	salt cation−anion	expt. E (V) (V vs Li^+/Li)	comp. OCV. (V) without counteranion	comp. OCV. (V) with counteranion
TEMPO	ETC	$LiPF_6$	3.58[22]	3.57	3.55
PROXYL	ETC	$LiPF_6$	3.6[24]	3.57	3.55
spirobisnitroxide	MeCH	$LiPF_6$	3.68 (4.43)[26]	3.71 (4.46)	3.66 (4.40)
nitronylnitroxide	MeCH	$(R)_4NClO_4$	3.60[25]	3.66	3.63

DOI: 10.1021/acs.jpcc.5b07886
J. Phys. Chem. C 2015, 119, 23373−23378

CONCLUSIONS

The ΔSCF technique based on DFT calculations with the B3LYP exchange-correlation functional and the medium size basis set 6-31+G* associated with the SMD polarizable continuum model has been demonstrated to be a fast method to accurately predict the redox potentials of organic radicals. This method makes it possible to reproduce the shift in reduction potentials when changing various functional groups of a given molecule. On the basis of these conclusions, this approach could be applied to hundreds or thousands of theoretically designed radicals to perform a high-throughput computational screening. The best candidates could be identified to guide the experimental search according to the desired open-cell voltage depending on specific battery applications.

AUTHOR INFORMATION

Corresponding Author

*Phone: +32 (0)10 479623. Fax: +32(0)10 473102. E-mail: gian-marco.rignanese@uclouvain.be.

Notes

The authors declare no competing financial interest.

ACKNOWLEDGMENTS

We thank Prof. Denis Jacquemin for performing the CCSD calculations reported in the present manuscript. N.D., G.H., J.-C.C., and G.-M.R. acknowledge the National Fund for Scientific Research [F.R.S.-FNRS] of Belgium for financial support. This research is connected to the BATWAL project sponsored by the Communauté Wallonie-Bruxelles. Computational resources were provided by the supercomputing facilities of the Université catholique de Louvain (CISM/UCL) and the Consortium des Equipements de Calcul Intensif en Fédération Wallonie-Bruxelles (CECI). X.B. acknowledges support from the French national funding agency (ANR) under contract PANELS ANR-12-BS04-0001 and from the GENCI national supercomputing agency (CURIE center) under contract no. i2012096655.

REFERENCES

(1) Tarascon, J.-M.; Armand, M. Issues and Challenges Facing Rechargeable Lithium Batteries. *Nature* **2001**, *414*, 359−367.

(2) Poizot, P.; Dolhem, F. Clean Energy New Deal for a Sustainable World: from non-CO2 Generating Energy Sources to Greener Electrochemical Storage Devices. *Energy Environ. Sci.* **2011**, *4*, 2003−2019.

(3) Liang, Y.; Tao, Z.; Chen, J. Organic Electrode Materials for Rechargeable Lithium Batteries. *Adv. Energy Mater.* **2012**, *2*, 742−769.

(4) Song, Z.; Zhou, H. Towards Sustainable and Versatile Energy Storage Devices: an Overview of Organic Electrode Materials. *Energy Environ. Sci.* **2013**, *6*, 2280−2301.

(5) Janoschka, T.; Hager, M.; Schubert, U. Powering up the Future: Radical Polymers for Battery Applications. *Adv. Mater.* **2012**, *24*, 6397−6409.

(6) Nakahara, K.; Iwasa, S.; Satoh, M.; Morioka, Y.; Iriyama, J.; Suguro, M.; Hasegawa, E. Rechargeable Batteries with Organic Radical Cathodes. *Chem. Phys. Lett.* **2002**, *359*, 351−354.

(7) Suga, T.; Pu, Y.-J.; Kasatori, S.; Nishide, H. Cathode- and Anode-Active Poly(nitroxylstyrene)s for Rechargeable Batteries: p- and n-Type Redox Switching via Substituent Effects. *Macromolecules* **2007**, *40*, 3167−3173.

(8) Vlad, A.; Singh, N.; Rolland, J.; Melinte, S.; Ajayan, P. M.; Gohy, J.-F. Hybrid Supercapacitor-Battery Materials for Fast Electrochemical Charge Storage. *Sci. Rep.* **2014**, *4*, 4315.

(9) Bachman, J. E.; Curtiss, L. A.; Assary, R. S. Investigation of the Redox Chemistry of Anthraquinone Derivatives Using Density Functional Theory. *J. Phys. Chem. A* **2014**, *118*, 8852−8860.

(10) Hachmann, J.; Olivares-Amaya, R.; Jinich, A.; Appleton, A. L.; Blood-Forsythe, M. A.; Seress, L. R.; Román-Salgado, C.; Trepte, K.; Atahan-Evrenk, S.; Er, S.; et al. Lead Candidates for High-Performance Organic Photovoltaics from High-Throughput Quantum Chemistry - the Harvard Clean Energy Project. *Energy Environ. Sci.* **2014**, *7*, 698−704.

(11) Chen, H.; Hautier, G.; Jain, A.; Moore, C.; Kang, B.; Doe, R.; Wu, L.; Zhu, Y.; Tang, Y.; Ceder, G. Carbonophosphates: A New Family of Cathode Materials for Li-Ion Batteries Identified Computationally. *Chem. Mater.* **2012**, *24*, 2009−2016.

(12) Meng, Y. S.; Arroyo-de Dompablo, M. E. Recent Advances in First Principles Computational Research of Cathode Materials for Lithium-Ion Batteries. *Acc. Chem. Res.* **2013**, *46*, 1171−1180.

(13) Hautier, G.; Jain, A.; Mueller, T.; Moore, C.; Ong, S. P.; Ceder, G. Designing Multielectron Lithium-Ion Phosphate Cathodes by Mixing Transition Metals. *Chem. Mater.* **2013**, *25*, 2064−2074.

(14) Jain, A.; Hautier, G.; Ong, S. P.; Dacek, S.; Ceder, G. Relating Voltage and Thermal Safety in Li-Ion Battery Cathodes: a High-Throughput Computational Study. *Phys. Chem. Chem. Phys.* **2015**, *17*, 5942−5953.

(15) Kohn, W.; Sham, L. J. Self-Consistent Equations Including Exchange and Correlation Effects. *Phys. Rev.* **1965**, *140*, A1133−1138.

(16) Hohenberg, P.; Kohn, W. Inhomogeneous Electron Gas. *Phys. Rev.* **1964**, *136*, B864−871.

(17) Marenich, A. V.; Cramer, C. J.; Truhlar, D. G. Universal Solvation Model Based on Solute Electron Density and on a Continuum Model of the Solvent Defined by the Bulk Dielectric Constant and Atomic Surface Tensions. *J. Phys. Chem. B* **2009**, *113*, 6378−6396.

(18) Hedin, L. New Method for Calculating the One-Particle Green's Function with Application to the Electron-Gas Problem. *Phys. Rev.* **1965**, *139*, A796−A823.

(19) Hybertsen, M. S.; Louie, S. G. Electron Correlation in Semiconductors and Insulators: Band Gaps and Quasiparticle Energies. *Phys. Rev. B: Condens. Matter Mater. Phys.* **1986**, *34*, 5390−5413.

(20) Godby, R. W.; Schlüter, M.; Sham, L. J. Self-Energy Operators and Exchange-Correlation Potentials in Semiconductors. *Phys. Rev. B: Condens. Matter Mater. Phys.* **1988**, *37*, 10159−10175.

(21) Onida, G.; Reining, L.; Rubio, A. Electronic Excitations: Density-Functional versus Many-Body Green's-Function Approaches. *Rev. Mod. Phys.* **2002**, *74*, 601−659.

(22) Nishide, H.; Suga, T. Organic Radical Battery. *Electrochem. Soc. Interface* **2005**, *14*, 32−36.

(23) Frisch, M. J.; Trucks, G. W.; Schlegel, H. B.; Scuseria, G. E.; Robb, M. A.; Cheeseman, J. R.; Scalmani, G.; Barone, V.; Mennucci, B.; Petersson, G. A.; et al. *Gaussian 09*, revision D.01.; Gaussian, Inc.: Wallingford, CT, 2009.

(24) Qu, J.; Katsumata, T.; Satoh, M.; Wada, J.; Masuda, T. Synthesis and Properties of Polyacetylene and Polynorbornene Derivatives Carrying 2,2,5,5-Tetramethyl-1-pyrrolidinyloxy Moieties. *Macromolecules* **2007**, *40*, 3136−3144.

(25) Suga, T.; Sugita, S.; Ohshiro, H.; Oyaizu, K.; Nishide, H. p- and n-Type Bipolar Redox-Active Radical Polymer: Toward Totally Organic Polymer-Based Rechargeable Devices with Variable Configuration. *Adv. Mater.* **2011**, *23*, 751−754.

(26) Nesvadba, P.; Bugnon, L.; Maire, P.; Novák, P. Synthesis of A Novel Spirobisnitroxide Polymer and its Evaluation in an Organic Radical Battery. *Chem. Mater.* **2010**, *22*, 783−788.

(27) Marenich, A. V.; Ho, J.; Coote, M. L.; Cramer, C. J.; Truhlar, D. G. Computational Electrochemistry: Prediction of Liquid-Phase Reduction Potentials. *Phys. Chem. Chem. Phys.* **2014**, *16*, 15068−15106.

(28) Kim, K.; Jordan, K. D. Comparison of Density Functional and MP2 Calculations on the Water Monomer and Dimer. *J. Phys. Chem.* **1994**, *98*, 10089−10094.

DOI: 10.1021/acs.jpcc.5b07886
J. Phys. Chem. C 2015, 119, 23373−23378

(29) Stephens, P. J.; Devlin, F. J.; Chabalowski, C. F.; Frisch, M. J. Ab Initio Calculation of Vibrational Absorption and Circular Dichroism Spectra Using Density Functional Force Fields. *J. Phys. Chem.* **1994**, *98*, 11623−11627.
(30) Perdew, J. P.; Ernzerhof, M.; Burke, K. Rationale for Mixing Exact Exchange with Density Functional Approximations. *J. Chem. Phys.* **1996**, *105*, 9982−9985.
(31) Adamo, C.; Barone, V. Toward Reliable Density Functional Methods without Adjustable Parameters: The PBE0Model. *J. Chem. Phys.* **1999**, *110*, 6158−6170.
(32) Perdew, J. P.; Burke, K.; Ernzerhof, M. Generalized Gradient Approximation Made Simple. *Phys. Rev. Lett.* **1996**, *77*, 3865−3868.
(33) Perdew, J. P.; Burke, K.; Ernzerhof, M. Generalized Gradient Approximation Made Simple [Phys. Rev. Lett. 77, 3865 (1996)]. *Phys. Rev. Lett.* **1997**, *78*, 1396−1396.
(34) Meng, Y.; Wu, Y.; Hwang, B.; Li, Y.; Ceder, G. Combining Ab Initio Computation with Experiments for Designing New Electrode Materials for Advanced Lithium Batteries: LiNi 1/3Fe 1/6Co 1/6Mn 1/3O 2. *J. Electrochem. Soc.* **2004**, *151*, A1134−A1140.
(35) Assary, R. S.; Curtiss, L. A.; Redfern, P. C.; Zhang, Z.; Amine, K. Computational Studies of Polysiloxanes: Oxidation Potentials and Decomposition Reactions. *J. Phys. Chem. C* **2011**, *115*, 12216−12223.
(36) Ong, S. P.; Andreussi, O.; Wu, Y.; Marzari, N.; Ceder, G. Electrochemical Windows of Room-Temperature Ionic Liquids from Molecular Dynamics and Density Functional Theory Calculations. *Chem. Mater.* **2011**, *23*, 2979−2986.
(37) Psciuk, B. T.; Lord, R. L.; Munk, B. H.; Schlegel, H. B. Theoretical Determination of One-Electron Oxidation Potentials for Nucleic Acid Bases. *J. Chem. Theory Comput.* **2012**, *8*, 5107−5123.
(38) Burkhardt, S. E.; Lowe, M. A.; Conte, S.; Zhou, W.; Qian, H.; Rodríguez-Calero, G. G.; Gao, J.; Hennig, R. G.; Abruña, H. D. Tailored Redox Functionality of Small Organics for Pseudocapacitive Electrodes. *Energy Environ. Sci.* **2012**, *5*, 7176−7187.
(39) Burkhardt, S. E.; Bois, J.; Tarascon, J.-M.; Hennig, R. G.; Abruña, H. D. Li-Carboxylate Anode Structure-Property Relationships from Molecular Modeling. *Chem. Mater.* **2013**, *25*, 132−141.
(40) Assary, R. S.; Brushett, F. R.; Curtiss, L. A. Reduction Potential Predictions of Some Aromatic Nitrogen-Containing Molecules. *RSC Adv.* **2014**, *4*, 57442−57451.
(41) Ceder, G.; Hautier, G.; Jain, A.; Ong, S. Recharging Lithium Battery Research with First-Principles Methods. *MRS Bull.* **2011**, *36*, 185−191.
(42) Aydinol, M. K.; Kohan, A. F.; Ceder, G.; Cho, K.; Joannopoulos, J. *Ab initio* Study of Lithium Intercalation in Metal Oxides and Metal Dichalcogenides. *Phys. Rev. B: Condens. Matter Mater. Phys.* **1997**, *56*, 1354−1365.
(43) Blase, X.; Attaccalite, C.; Olevano, V. First-Principles GW Calculations for Fullerenes, Porphyrins, Phtalocyanine, and other Molecules of Interest for Organic Photovoltaic Applications. *Phys. Rev. B: Condens. Matter Mater. Phys.* **2011**, *83*, 115103.
(44) Faber, C.; Attaccalite, C.; Olevano, V.; Runge, E.; Blase, X. First-Principles GW Calculations for DNA and RNA Nucleobases. *Phys. Rev. B: Condens. Matter Mater. Phys.* **2011**, *83*, 115123.
(45) Blase, X.; Attaccalite, C. Charge-Transfer Excitations in Molecular Donor-Acceptor Complexes within the Many-Body Bethe-Salpeter Approach. *Appl. Phys. Lett.* **2011**, *99*, 171909.
(46) Valiev, M.; Bylaska, E. J.; Govind, N.; Kowalski, K.; Straatsma, T. P.; van Dam, H. J. J.; Wang, D.; Nieplocha, J.; Apra, E.; Windus, T. L.; et al. NWChem: A Comprehensive and Scalable Open-Source Solution for Large Scale Molecular Simulations. *Comput. Phys. Commun.* **2010**, *181*, 1477−1489.
(47) Dunning, T. H. Gaussian Basis Sets for Use in Correlated Molecular Calculations. I. The Atoms Boron through Beon and Hydrogen. *J. Chem. Phys.* **1989**, *90*, 1007−1023.
(48) Papajak, E.; Leverentz, H. R.; Zheng, J.; Truhlar, D. G. Efficient Diffuse Basis Sets: cc-pVxZ+ and maug-cc-pVxZ. *J. Chem. Theory Comput.* **2009**, *5*, 1197−1202.
(49) Papajak, E.; Truhlar, D. G. Efficient Diffuse Basis Sets for Density Functional Theory. *J. Chem. Theory Comput.* **2010**, *6*, 597−601.
(50) Weigend, F.; Köhn, A.; Hättig, C. Efficient Use of the Correlation Consistent Basis Sets in Resolution of the Identity MP2 Calculations. The. *J. Chem. Phys.* **2002**, *116*, 3175−3183.
(51) Bruneval, F.; Marques, M. A. L. Benchmarking the Starting Points of the GW Approximation for Molecules. *J. Chem. Theory Comput.* **2013**, *9*, 324−329.
(52) Körbel, S.; Boulanger, P.; Duchemin, I.; Blase, X.; Marques, M. A. L.; Botti, S. Benchmark Many-Body GW and BetheSalpeter Calculations for Small Transition Metal Molecules. *J. Chem. Theory Comput.* **2014**, *10*, 3934−3943.
(53) Isse, A. A.; Gennaro, A. Absolute Potential of the Standard Hydrogen Electrode and the Problem of Interconversion of Potentials in Different Solvents. *J. Phys. Chem. B* **2010**, *114*, 7894−7899.
(54) Bruneval, F. GW Approximation of the Many-Body Problem and Changes in the Particle Number. *Phys. Rev. Lett.* **2009**, *103*, 176403.

DOI: 10.1021/acs.jpcc.5b07886
J. Phys. Chem. C 2015, 119, 23373−23378